Microwave-assisted Method for Synthesis of Cassava Starch-Grafted Polyacrylamide Hydrogel: Initiator and Irradiation Power Variation

Maudy Pratiwi Novia Matovanni
Department of Chemical Engineering, Faculty of Engineering, Universitas Sebelas Maret

Distantina, Sperisa
Department of Chemical Engineering, Faculty of Engineering, Universitas Sebelas Maret

Kaavessina, Mujtahid
Department of Chemical Engineering, Faculty of Engineering, Universitas Sebelas Maret

Fadilah
Department of Chemical Engineering, Faculty of Engineering, Universitas Sebelas Maret

https://doi.org/10.5109/7160873

出版情報：Evergreen. 10 (4), pp.2134-2144, 2023-12. 九州大学グリーンテクノロジー研究教育センター
バージョン：

Microwave-assisted Method for Synthesis of Cassava Starch-Grafted Polyacrylamide Hydrogel: Initiator and Irradiation Power Variation

Maudy Pratiwi Novia Matovanni[1], Sperisa Distantina[1,*], Mujtahid Kaavessina[1], and Fadilah[1]

[1]Department of Chemical Engineering, Faculty of Engineering, Universitas Sebelas Maret, Jl. Ir. Sutami 36A, Kentingan, Surakarta 57126, Indonesia

*Author to whom correspondence should be addressed:
E-mail: sperisa_distantina@staff.uns.ac.id

(Received January 4, 2023; Revised September 11, 2023; accepted October 22, 2023)

Abstract: This study aimed to synthesize cassava starch-grafted polyacrylamide hydrogel (CS-g-PAM) by the microwave-assisted method based on cassava starch as the backbone, acrylamide as the monomer, and potassium peroxodisulfate (KPS) as the initiator. In this paper, the effect of KPS amount as initiator and microwave irradiation power was investigated on the obtained hydrogel properties as a candidate for enhanced oil recovery (EOR) application. Fourier-transform infrared (FTIR), scanning electron microscopy (SEM), X-ray powder diffraction (XRD), and thermogravimetric analysis (TGA) were used to investigate the effective grafting of polyacrylamide chains onto the backbone of cassava starch. Results show that the preparation of CS-g-PAM with 0.3 g of KPS and 700 W of irradiation power resulted in the best performance, which was 602.66% of grafting percentage and 81.72% of water solubility. Its viscosity also exceeded 96% after 15 days of aging.

Keywords: hydrogel; microwave-assisted method; potassium peroxodisulfate; enhanced oil recovery

1. Introduction

Hydrogel is commonly used in mature reservoirs due to its excellent profile control, simplicity of manufacture, and capacity to minimize excessive permeability[1)]. Because of their longevity, eco-friendliness, economic efficiency, high sweep efficiency, high comfort and handling of hydrogel injection operations, and positive results across the world, the usage of hydrogel as polymer injection agents in improving oil production has risen[2)].

Polyacrylamide (PAM), partially hydrolyzed polyacrylamide (HPAM), and its derivatives are the most often utilized polymers in oil fields because of their strong shear strength and thickening ability[3)]. However, it has major limitations owing to acrylamide functional group hydrolysis, such as high temperature and salinity sensitivity. High temperatures produced hydrolysis, which increased chain shrinkage and lowered viscosity. In high salinity solutions, the charges of the carboxyl groups are neutralized, causing the polymer chain to shorten and the viscosity to drop[4)]. Because of the toxicity and carcinogenicity of the leftover monomers, the usage of synthetic polymers has a detrimental impact on the environment[5)]. To overcome these problems, several studies have reported that the grafting process of synthetic polymers on natural polymers such as polysaccharides can improve the hydrogel properties produced[6–8)].

Polysaccharides, such as cassava starch, offer strong temperature and salinity tolerance as a natural and renewable raw material with plentiful supplies and no pollution. Because of their helical form, natural polymers are more resistant to salt and temperature than synthetic polymers[5,9)]. Natural polymers are also inexpensive, abundantly available, biocompatible, and environmentally friendly, but have limited biodegradation and structural modification properties due to their complex structure[10)].

As a result, hydrogel synthesis from a mixture of natural and synthetic polymers can be an ecologically benign, low-cost option with high reservoir resistance. Hydrogel from a combination of natural and synthetic polymers with excellent resistance properties in high salinity and temperature is used in water treatment[11,12)], sorbents for the removal of heavy metal ions and waste dyes[10,13,14)], carriers for functional food additives or drugs[15)], controlled release fertilizer[16,17)], and agents in enhanced oil recovery[18,19)].

Previous research[20)] studied the synthesis of hydrogels from milk protein casein and acrylamide by grafting

method using microwaves. Wu et al.[21] studied the synthesis of hydrogels from chitosan, acrylamide, and acryloyloxyethyl trimethylammonium chloride by grafting method using microwaves and the initiator of 2,2'-azobis dihydrochloride. Mishra and Kundu[22] studied the synthesis of hydrogels from fenugreek gum and acrylamide using microwaves and ceric ammonium nitrate as an initiator. Referring to several previous studies, the grafting method can be done using the microwave-assiassisted method. When compared with conventional heating methods, the use of microwaves speeds the synthesis of hydrogel, resulting in more polymer products in a short period of time. The microwave intensity and irradiation exposure period are electronically regulated to control the percentage of grafting[23].

Grafting was carried out in this investigation employing microwave radiation and potassium peroxodisulfate (KPS) as an initiator. The produced hydrogel, CS-g-PAM hydrogel, might be a prospect for enhanced oil recovery (EOR) application. In this study, we investigated the impact of the KPS/cassava starch weight ratio and irradiation power on the tolerance of reservoir properties of CS-g-PAM obtained as a thickening agent, as evidenced by the swelling ratio and viscosity under reservoir conditions, in addition to the viscosity resistance of the polymer solution for 15 days. Fourier-transform infrared (FTIR), scanning electron microscopy (SEM), X-ray powder diffraction (XRD), and thermogravimetric analysis (TGA) were used to assess the effective grafting of polyacrylamide chains onto the backbone of cassava starch.

2. Experimental Section

2.1 Materials

The cassava starch (CS) for the backbone was sourced from a local market in Surakarta, Indonesia. E. Merck, Germany, supplied the monomer acrylamide (AM) (>99%) and the initiator potassium peroxydisulfate (KPS) (>99%). Saba Kimia in Surakarta, Indonesia, supplied the acetone (technical). All chemicals and reagents are utilized without further processing

2.2 Synthesis of CS-g-PAM

CS-g-PAM was synthesized by modifying the KPS amount and power of irradiation, as shown in Tabel 1. In 50 mL of distilled water, cassava starch, acrylamide, and KPS were added. The solution mixture was placed in a 1000 mL beaker and microwaved (Krisbow 20 L) at 364 W. The solution was microwaved for 30 seconds until it reached 70°C boiling point, then cooled by putting the reaction beaker in cold water. The cycle of irradiation-cooling was repeated until 180 seconds, or 6 cycles.

After the grafting process by microwave-assisted method was done, the gel material was left to stand for 24 hours to complete the grafting reaction process. Excess acetone was absorbed into the reaction beaker's gel material until a precipitate occurred. The CS-g-PAM precipitate was dried in an oven at 50°C for 24 hours. The percentage of grafting of CS-g-PAM obtained was calculated by Eq 1.

$$\%\text{grafting} = \frac{(\text{mass of CS} - \text{g} - \text{PAM}) - (\text{mass of CS})}{\text{mass of CS}} \, x \, 100\% \quad (1)$$

2.3 Fourier-Transform Infrared Spectroscopy (FTIR)

On a Frontier FTIR spectrophotometer (Shimadzu, IRSpirit), the FTIR spectra of cassava starch and CS-g-PAM (A - E) were studied. Without producing pellets with KBr, CS-g-PAM produced under various circumstances was examined directly.

2.4 Scanning Electron Microscopy (SEM)

JEOL Benchtop Scanning Electron Microscopy JCM 7000 was used to evaluate the surface microstructure of cassava starch and CS-g-PAM (A - E). The gold-coated specimens were examined under magnifications ranging from 500 to 5000x. Before SEM analysis, cassava starch was gelatinized.

Table 1. Variation comnditions for the synthesis of CS-g-PAM hydrogel

Code	Mass of CS (g)	Mass of AM (g)	Mass of KPS (g)	Irradiation time (s)	Irradiation power (W)	%grafting
A	1	5	0.1	180	364	104.70
B	1	5	0.3	180	364	575.58
C	1	5	0.5	180	364	592.58
D	1	5	0.3	180	511	593.98
E	1	5	0.3	180	700	602.66

2.5 X-ray powder diffraction (XRD)

XRD spectra of cassava starch and CS-g-PAM were collected to identify the crystallinity of cassava

starch and CS-g-PAM to explore structural differences before and after grafting process. The XRD pattern of the samples was recorded using a XRD MD10 minidiffractometer, MTI. Scans were run from 17 to 71°C. The instrument was operated with CuKα monochromatic radiation (λ= 1.4518 °A).

2.6 Thermogravimetric Analysis (TGA)

Thermal properties of cassava starch and CS – g – PAM samples were studied by TGA. Linseis STA PT1600 (Germany) was used to test the thermal stability between cassava starch and CS-g-PAM samples. Temperature set from 25 to 500ºC and the constant heating rate was 10ºC/min.

2.7 Swelling test

The weight of the dried CS-g-PAM was recorded as W_1 (grams). The swelling test was investigated by soaking W_1 in 100 mL of distilled water with varied swelling periods, NaCl concentrations, and temperatures based on reservoir conditions. The swollen CS-g-PAM was represented as W_2 (grams). Eq 2 was used to determine the swelling ratio.

$$S = \frac{W_2 - W_1}{W_1} \qquad (2)$$

2.8 Water Solubility Measurement

1 g of CS-g-PAM was dissolved in 100 mL of distilled water for 1 hour before being filtered. The precipitated filter paper was dried to a consistent weight in an air oven at 50°C. Eq 3 was used to compute the percentage of CS-g-PAM solubility in water. The starting weight of the CS-g-PAM (1 g) was W_0, and the weight of dried precipitated CS-g-PAM was W_i.

$$\text{Water solubility } \% = \frac{W_0 - W_i}{W_0} x100\% \quad (3)$$

2.9 Thickening Ability

The powdered CS-g-PAM was dissolved in distilled water at room temperature. Based on reservoir conditions, the viscosity of 1wt% polymer solutions was measured at varied NaCl concentrations and temperatures. The Brookfield Viscometer DV2T was used to test the viscosity of the polymer solution.

2.10 Anti-aging Ability

The viscosity of polymer solutions with a 1wt% concentration was tested in distilled water for 15 days. The observed viscosity was determined using a Brookfield Viscometer DV2T. Viscosity retention was calculated by Eq 4 with η_{15} was viscosity after aging and η_1 was initial viscosity.

$$\text{Viscosity retention rate} = \frac{\eta_{15}}{\eta_1} \text{x} 100\% \qquad (4)$$

3. Result And Discussion

3.1 Synthesis of Cassava Starch-grafted Polyacrylamide (CS-g-PAM)

The conditions for the synthesis of cassava starch-polyacrylamide (CS-g-PAM) hydrogel are shown in Table 1. Synthesis of CS-g-PAM was performed by microwave-assisted method. Potassium peroxodisulfate (KPS) was used as an initiator in this reaction. The weight ratio of KPS/cassava starch used affects the grafting percentage of CS-g-PAM . CS-g-PAM A, B, and C showed the higher the number of KPS used, the higher the percentage of grafting produced. The increase in grafting percentage was caused by the availability of free radicals generated in the cassava starch backbone by the initiator. The highest grafting percentage of 592.58% for CS-g-PAM was attained with 5/10 weight ratio of KPS/cassava starch.

The mechanism of microwave-assisted grafting by which KPS generates free radical affected by initiator concentration and power radiation. When polar molecules are irradiated in a microwave, they produce rotation of the molecules, causing the generation of heat. In this case, the heat in the microwave is absorbed by the existing polar groups (for example -OH groups attached to the polysaccharide backbone) and as a result, bond breaking occurs, which leads to the formation of free radical sites. KPS generates free radicals is believed to absorbed by the water molecules is quickly transferred to the acrylamide molecules, resulting in the breaking of the double bonds, thus producing another set of free radicals. This effect produces free radicals in the -OH groups of the polysaccharide backbone and in acrylamide, the free radicals formed then recombine with each other through initiation, propagation and termination steps to produce graft copolymers.

The grafting percentage in CS-g-PAM B, D, and E is affected by the irradiation applied. As the irradiation power increased from 364 to 700 W, the grafting percentage increased. This was owing to the increased availability of microwave energy at higher microwave power, which resulted in the synthesis of more macroradicals and a high grafting percentage [24]. The optimum grafting percentage of 602.66% for CS-g-PAM was attained with 700 W irradiation power.

3.2 Fourier-Transform Infrared Spectroscopy (FTIR)

The FTIR results of cassava starch, acrylamide and CS-g-PAM are depicted in Fig. 1. The FTIR results of cassava starch showed that the main absorption peaks were: 3292 cm^{-1} (O-H strain vibration), 2933 cm^{-1} (C-H strain vibration), and 1152 cm^{-1}, 1078 cm^{-1}, 1016 cm^{-1} shows the C-O-C strain vibration. FT-IR results of acrylamide showed the main absorption peaks, including 3359 cm^{-1} and 3173 cm^{-1} (asymmetric and symmetrical extension of the N-H bond), 1676 cm^{-1} (C=O strain vibration), 1607 cm^{-1} (N-H strain vibration of -$CO-NH_2$), 1422 cm^{-1} (C-N streching), and 960 cm^{-1} (C-H strain).

In Fig. 1, it can be seen that all grafted CS-g-PAM (A – E) display identical profiles in the FTIR spectrum. This proves that variations in the weight ratio of KPS/cassava starch and irradiation power produce the same product. Therefore, the discussion was carried out using the CS-g-PAM A as a representative for all grafted samples.

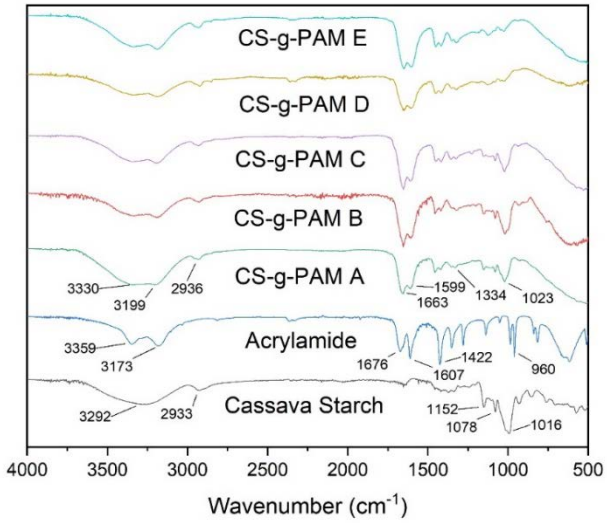

Fig 1: FTIR Spectra of cassava starch, acrylamide, and CS-g-PAM (A – E)

In CS-g-PAM A, the O-H strain vibration of the starch hydroxyl group overlaps with the N-H strain vibration of the PAM amide group, resulting in a peak at 3330 cm^{-1} and a shoulder peak at 3199 cm^{-1}. The C-H strain vibration is related to the tiny peak at 2936 cm^{-1}. The C-O-C strain vibration is given the band at 1023 cm^{-1}. The formation of a sharp peak at 1663 cm^{-1} was related with C = O stretching, while the appearance of a sharp peak at 1599 cm^{-1} was connected with N-H stretching (ie amide I and amide II stretching). In addition, there is another peak in the graft product at 1334 cm^{-1}, showing C-N stretching. The existence of strain vibrations C=O, N-H, and C-N at $-CONH_2$ suggests that the grafting procedure was successful.

According to the FTIR spectra in Fig. 1, CS-g-PAM are created as a result of free radicals generated in the cassava starch backbone with acrylamide through the use of the free radical reaction process. Because the O-H group in CS-g-PAM is replaced by a polyacrylamide chain, the peak of the O-H group is not as sharp as that of cassava starch[25].

3.3 Scanning Electron Microscopy (SEM)

The results of SEM characterization of cassava starch, acrylamide, and CS-g-PAM are shown in Fig. 2. The results of the SEM test showed that there were differences in surface shape between cassava starch (CS), acrylamide (AM), and CS-g-PAM (A – E).

The gelatinized cassava starch displayed a smooth surface. Following the grafting process, CS-g-PAM exhibits a coarse and multi-layered folded structure. According to the SEM observations, the addition of grafted monomers changed and deteriorated the surface structure of starch, possibly giving more active sites[12].

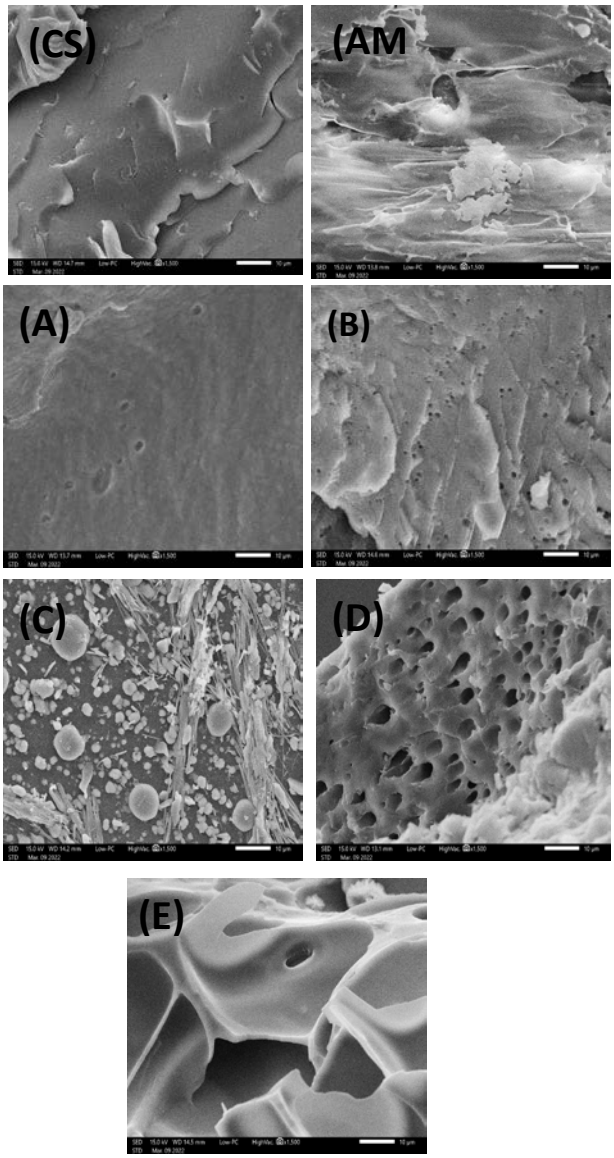

Fig. 2: SEM images of cassava starch (CS), acrylamide (AM), and CS-g-PAM (A – E)

In the morphology of CS-g-PAM A and B with increasing weight ratio of KPS/cassava starch from 1/10 to 3/10, more rough surfaces were seen. However, on CS-g-PAM C with a weight ratio of KPS/cassava starch was 5/10, granules with many irregularities and some connected parts were still visible. Increasing the weight ratio of KPS/cassava starch causes an excess of free radicals of cassava starch which combine to cause termination before monomer grafting[23]. Despite the grafting percentage of CS-g-PAM C being higher than CS-g-PAM A and B, the polyacrylamide grafted onto the backbone of cassava starch had shorter chains than the other products. Further, it will affect the properties obtained.

The morphology of CS-g-PAM B, D, and E with increasing irradiation power from 364 to 700 W showed a rougher surface and the presence of a large number of interconnected pores indicating a porous structure. As irradiation power increases, more free radicals are

generated, increasing the availability of graft sites [26]. Then more polyacrylamide will be grafted on cassava starch, causing more rough and porous surfaces on the morphological appearance.

Similar observations on the surface morphology of grafting product have been reported in starch-grafted flocculant (acrylamide and methacryloxyethyltrimethyl ammonium chloride)[12] and starch-grafted acrylamide[17]

3.4 X-ray powder diffraction Characterization (XRD)

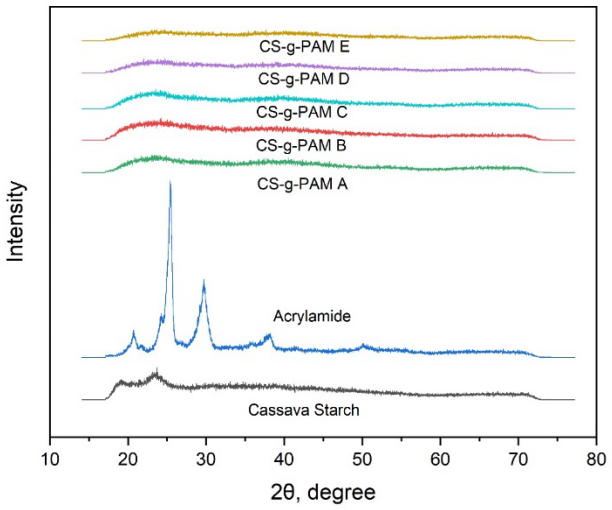

Fig. 3: XRD Spectra of cassava starch, acrylamide, and CS-g-PAM

The crystal structure of cassava starch, acrylamide, and CS-g-PAM was observed by XRD characterization to see the difference in the structure before and after the grafting process as shown in Fig. 3. As shown, two diffraction peaks existed near 18° and 23° registered for cassava starch. Similar observations on cassava starch diffraction peaks have been reported by You et al[27].

After grafting polyacrylamide, a drastic reduction in the crystallinity was observed. In the CS-g-PAM XRD spectrum, the peak of cassava starch at 2θ = 18° disappeared, while the peak intensity at 2θ = 23° was significantly reduced. The drop in crystallization peaks suggested that the graft copolymerization procedure disturbed the starch glucose ring structure, resulting in a reduction in the quantity of -OH groups. To some extent, reducing the -OH group inhibits intra and intermolecular hydrogen bonding[28]. Similar observations on the XRD trend of the grafting product have been reported by You et al[27] and Alharbi et al[16]. This indicates that cassava starch transformed into an amorphous substance, thereby proving the success of polyacrylamide grafting on the cassava starch backbone.

XRD diffractogram on acrylamide (AM) shows a crystal structure with characteristic peaks of 2θ = 20°, 25°, and 28°. These peaks indicate the crystalline nature of acrylamide. Similar results of crystalline peaks in acrylamide have been previously reported[29]. The AM peaks are entirely gone in CS-g-PAM. This implies that the final product has no leftover AM monomers[30].

3.5 Thermogravimetric Analysis (TGA)

The thermal stability of cassava starch and CS – g – PAM (A – E) are shown in Fig. 4. As seen in the graph when starch was synthesized into CS-g-PAM, its thermal stability improved, as evidenced by the quantity of remaining residue. The TGA curve for cassava starch exhibits a minor moisture loss at lower temperatures (below 100°C) and a considerable weight loss due to cassava starch degradation at around 310°C[17].

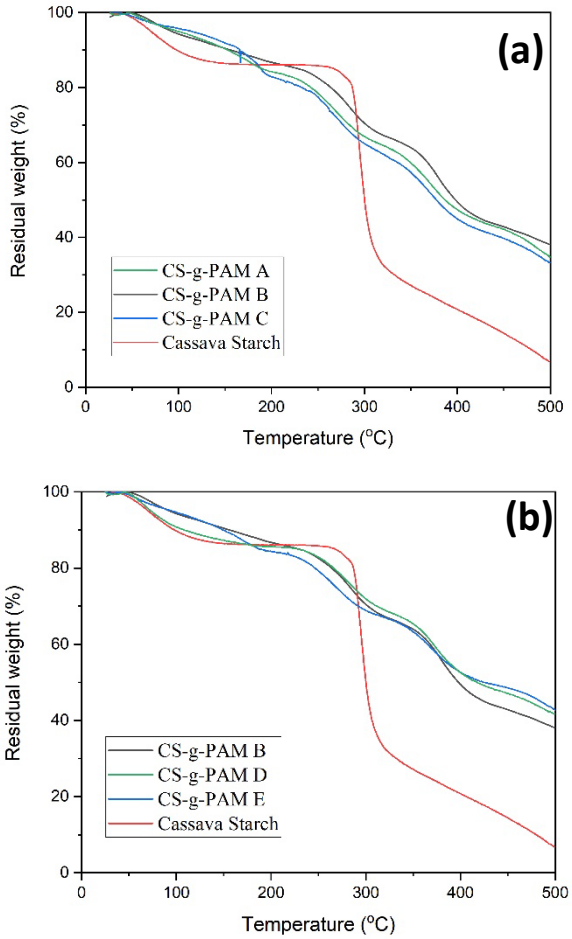

Fig. 4: TGA analysis of cassava starch and CS-g-PAM (a) effect of weight ratio of KPS/cassava starch (b) effect of irradiation power

Thermal stability of CS-g-PAM was enhanced when compared to cassava starch, resulting in three degradation phases beginning at roughly 100°C owing to moisture evaporation, 250°C due to grafted polymer degradation, and 350°C due to main polymer degradation[16].

Fig. 4(a) shows that the higher weight ratio of KPS/cassava starch from 1/10 to 3/10 resulted in higher quantity of remaining residue. However, increasing the weight ratio of KPS/cassava starch to 5/10 resulted in a decrease in the quantity of remaining residue due to a

decrease in the polyacrylamide chains from the grafted polymeric chains.

Fig. 4(b) shows that the higher irradiation power from 364 to 700 W resulted in a higher amount of left residue. It was due to more polyacrylamide will be grafted on cassava starch to increase irradiation power.

3.6 Swelling Test

The swelling ratio of CS-g-PAM in distillate water is depicted in Fig. 5, where the swelling ratio increases from 0 to 120 minutes of soaking. As shown in Fig. 5(a), the higher weight ratio of KPS/cassava starch from 1/10 to 3/10 resulted in a higher swelling ratio. However, when the weight ratio of KPS/cassava starch increased to 5/10, the swelling ratio decreased. The unique swelling performance of CS-g-PAM was related to the KPS/cassava starch ratio of 5/10 causing an excess of free radicals of cassava starch which causes faster termination, so that the polyacrylamide chain grafted on cassava starch is shorter and reduces the swelling ratio.

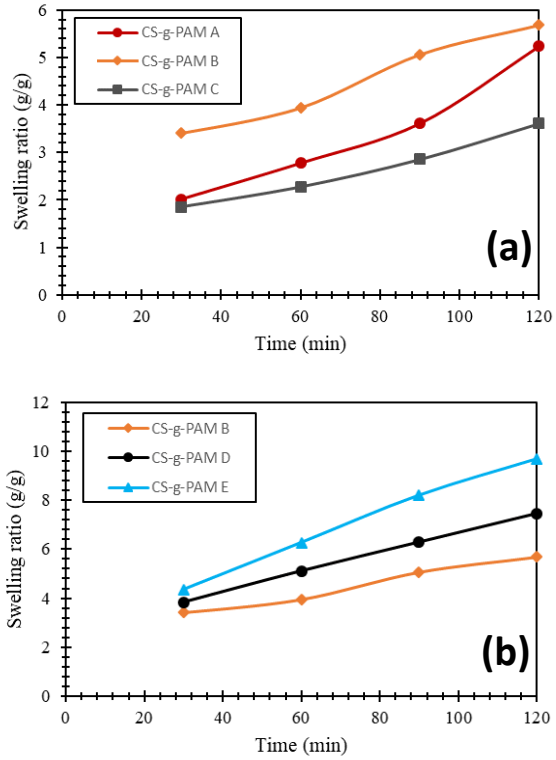

Fig. 5: Swelling ratio of CS-g-PAM in distilled water (a) effect of weight ratio KPS/cassava starch (b) effect of irradiation power

As shown in Fig. 5(b), the swelling ratio increased as irradiation power increased from 364 to 700 W. It was discovered that increasing the intensity of irradiation promotes the creation of more free radicals, resulting in more polyacrylamide grafted on cassava starch. This is also evident in the more rough and porous surfaces in the morphological appearance.

In actual reservoir conditions, salinity has a considerable impact on polymer characteristics. The swelling ratio was determined at different NaCl concentrations ranging from 0 to 250,000 ppm. Fig. 6 shows that the swelling ratio continued to decrease from 0 to 250,000 ppm NaCl concentration with an immersion time of 120 minutes. Increasing salt concentration causes electrostatic repulsion of the anions. The difference in ion concentration causes the osmotic pressure differential between the hydrogel network and the external solution to decrease[31].

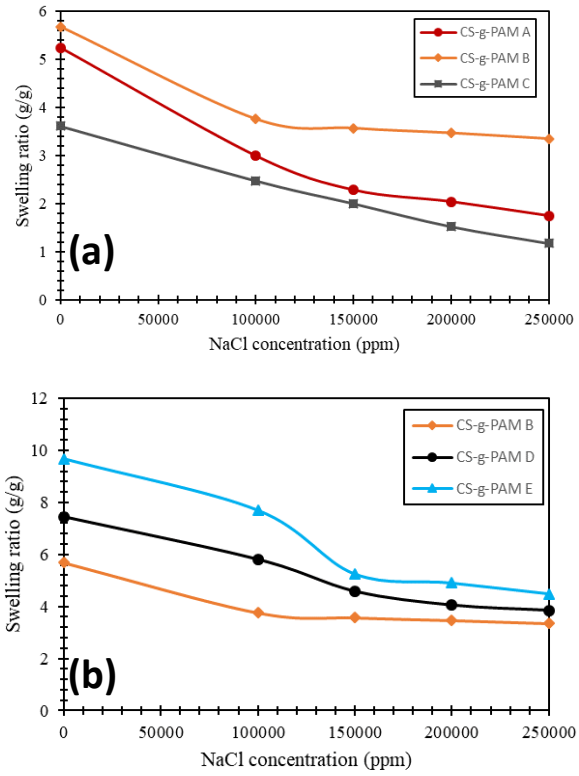

Fig. 6: Swelling ratio of CS-g-PAM at various NaCl concentration (a) effect of weight ratio KPS/cassava starch (b) effect of irradiation power

In previous study, the swelling ratio of Lutensol AT 25 E hydrogel and mathacrylate as CEOR agent at 200,000 ppm salinity was 1.4 g/g[32]. The swelling ratio of hydrogels of acrylamide, vinylpyrrolidone, and 2-acrylamido-2-methylpropane sulfonic sodium salt at a salinity of 250,000 ppm was 9.53 g/g[33]. CS-g-PAM has a swelling ratio in the range of 1 – 5 g/g at a NaCl concentration of 250,000 ppm. From the results of the swelling ratio of hydrogel that has been applied for EOR, It is evident that CS-g-PAM can be applied for EOR.

Fig. 7 shows that the swelling ratio is affected by temperature, where the swelling ratio continues to decrease from the temperature of 25 - 90°C. Hydrogen bonding has a major impact on the behavior of lowering the swelling ratio of CS-g-PAM in water. As temperature rises, hydrogen bond contacts weaken or dissolve, and hydrophobic carbon group interactions take control totally[34,35].

In the previous study, a similar result on the swelling ratio of acrylic acid and octadecyl acrylate hydrogel for plugging material in an oilfield continues to decrease from 1.8 g/g to 0.6 g/g from a temperature of 35 to 70°C[36]. Previous study has shown that CS-g-PAM may be used in EOR.

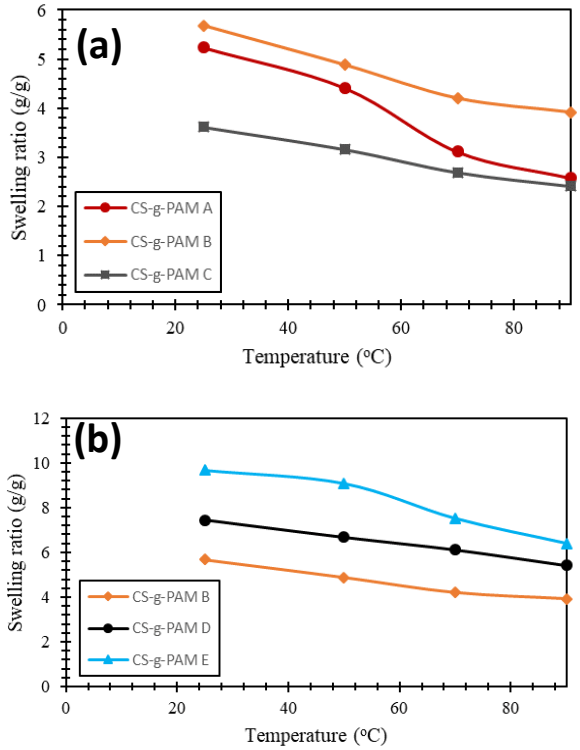

Fig 7: Swelling ratio of CS-g-PAM at various temperature (a) effect of weight ratio KPS/cassava starch (b) effect of irradiation power

3.7 Water Solubility Measurement

The results of the solubility of CS-g-PAM in water are presented in Table 2. The solubility of CS-g-PAM in water increased with increasing content of grafted polyacrylamide. Solubility in water increased from 63.62 to 81.72% with increasing irradiation power from 364 to 700 W. Solubility in water increased from 42.72 to 63.62% with increasing weight ratio of KPS/cassava starch from 1/10 to 1 /30, but when the weight ratio of KPS/cassava starch is 5/10, the solubility in water was 39.53%.

The inclusion of soluble polyacrylamide side chains and looser packing of cassava starch backbone chains may explain the enhanced water solubility of CS-g-PAM [15]. Increasing polyacrylamide chains grafted to cassava starch resulted in improved water solubility of CS-g-PAM obtained.

Table 2. Water Solubility of CS-g-PAM

CS-g-PAM	Water solubility (%)
A	42.72
B	63.62
C	39.53
D	71.23
E	81.72

3.8 Viscosity Test

The polymer solution can improve the viscosity of water and hence the effectiveness of oil sweep[37]. The viscosity of CS-g-PAM increased as the polymer solution content, as seen in Fig. 8. The internal friction of molecular motion rises with polymer concentration, leading to increased apparent viscosity and a dramatic increase in polymer solution viscosity[19]. As shown in Fig. 8(a), the viscosity of CS-g-PAM C was lower than that of CS-g-PAM A and B when the weight ratio of KPS/cassava starch was 5/10. The same trend was also shown with lower solubility compared to CS-g-PAM G and D.

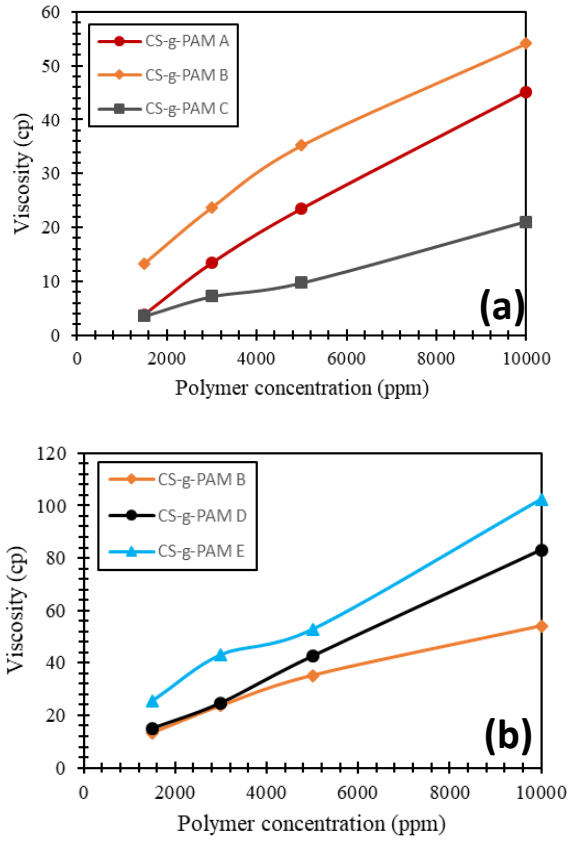

Fig. 8: Viscosity of CS-g-PAM (a) effect of weight ratio KPS/cassava starch (b) effect of irradiation power

According to Fig. 8(b), the polymer viscosity enhanced with increasing irradiation power because the integration of polyacrylamide increased the hydrodynamic volume of

CS-g-PAM in water, which could be attributed to acrylamide units breaking strong intra-hydrogen bonds[6].

The impact of NaCl content on the viscosity properties of the CS-g-PAM solution is depicted in Fig. 9. In all samples, CS-g-PAM lowered viscosity as the salt level increased. Because of the massive shock that enters the solution at lower salt concentrations, the viscosity of the solution reduces substantially. The impact of salt reduces as salt levels rise. At high salinity, the solution is salt-saturated, and additional salts have no effect on the polymer solution's structure[38]. The presence of electrolytes in the system modifies the polarity of the solution, resulting in electrostatic repulsion inside the molecule[19].

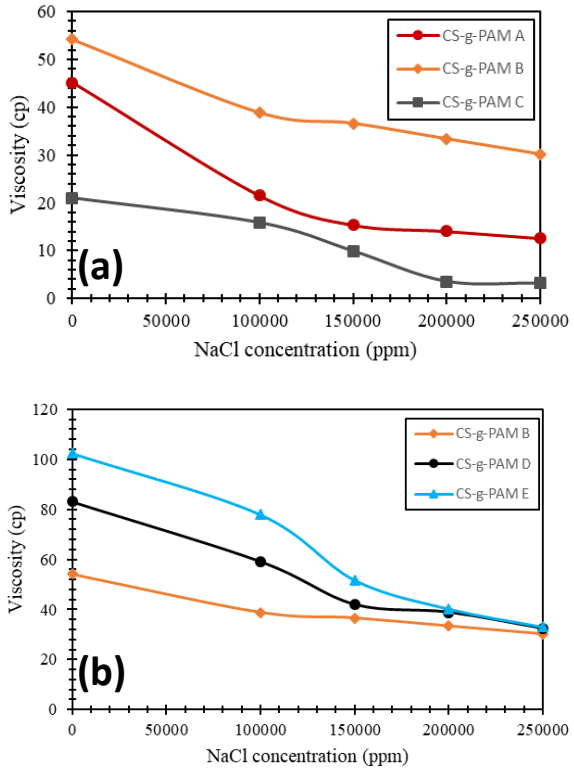

Fig. 9: Viscosity of CS-g-PAM at various NaCl concentrations (a) effect of weight ratio KPS/cassava starch (b) effect of irradiation power

Mellei et al[38] reported a similar discovery of lower viscosity of polymer solution in saline water. The influence of temperature on the viscosity of the CS-g-PAM polymer solution is depicted in Fig. 10. At high temperatures, CS-g-PAM is sensitive to hydrolysis, resulting in a reduction in viscosity. The breaking of strong intramolecular hydrogen bonds at high temperatures causes the viscosity to drop[6]. The functional groups that break the polymer in water are destroyed, leading in a decrease in solution viscosity[38].

Mellei et al[38] and Shehbaz et al[39] reported similar findings of reduced viscosity of polymer solution at high temperatures.

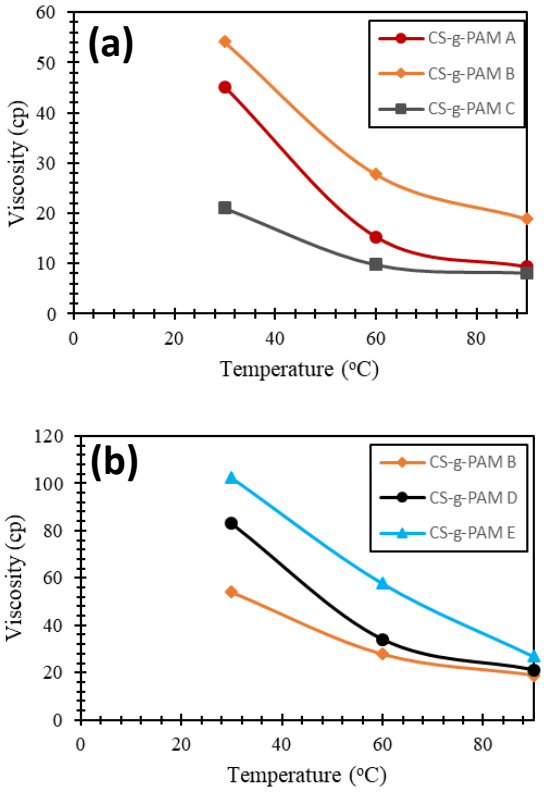

Fig. 10: Viscosity of CS-g-PAM at various temperature (a) effect of weight ratio KPS/cassava starch (b) effect of irradiation power

3.9 Anti-aging Test

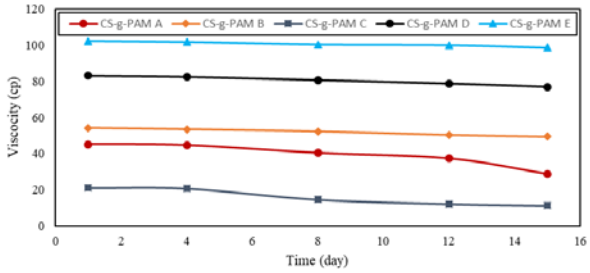

Fig. 11. Anti-aging result of CS-g-PAM

The capacity to avoid undesired changes in the chemical and physical composition of the polymer solution during application is referred to as anti-aging ability. Figure 11 depicts the viscosity of the CS-g-PAM solution in distillate water and at room temperature for 15 days. The viscosity of CS-g-PAM A on the 15th day was 63.80% of the viscosity on the first day. The viscosity of CS-g-PAM B on the 15th day was 91.24% of the viscosity on the first day. The viscosity of CS-g-PAM C on the 15th day was 53.05% of the viscosity on the first day. The viscosity of CS-g-PAM D on the 15th day was 92.61% of the viscosity on the first day. The viscosity of CS-g-PAM E on the 15th day was 96.43% of the viscosity on the first day. This shows that the weight ratio of KPS/cassava starch and irradiation power affect the anti-aging ability of CS-g-PAM produced.

Fig. 11 indicates that the incorporation of the weight ratio of KPS/cassava starch and irradiation power enhanced resistance to hydrolysis. The viscosity maintained stability till 15 days of aging. That proved that irradiation power of 700 W and weight ratio of KPS/cassava starch of 3/10 showed high improvement in gel performance. This is because more polyacrylamide grafted into cassava starch led to resistance to degradation by protecting the cassava starch from extensive biodegradation, which would otherwise result in a loss of viscosity.

4. Conclusion

The increase in the weight ratio of KPS/cassava starch caused an increase in grafting percentage, where the highest grafting yield was obtained when the weight ratio of KPS/cassava starch was 5:10. The swelling ratio, viscosity, water solubility, and anti-aging of the derived CS – g – PAM increased when the weight ratio of KPS/cassava starch was increased from 1:10 to 3:10. The swelling ratio, water solubility, anti-aging ability, and viscosity all reduced when the weight ratio of KPS/cassava starch was 5:10. The percentage of grafting increases as the irradiation power increases, with the maximum percentage grafting obtained when the irradiation power is 700 W. The swelling ratio, viscosity, water solubility, and anti-aging effectiveness of the resultant CS-g-PAM increase as the irradiation power increases. Considering the inexpensive of cassava starch, easy synthesis, and resistance of CS-g-PAM to various NaCl concentrations and temperatures according to reservoir conditions, CS-g-PAM can be a good candidate for EOR applications.

Acknowledgement

The authors would like to express their gratitude to the Indonesian Directorate General of Higher Education for financial support of this work under the Penelitian Fundamental 2022 PNBP Universitas Sebelas Maret with contract number 254/UN27.22/PT.01.03/2022.

References

1) M. B. Salehi, M. Soleimanian, and A. M. Moghadam, “Examination of disproportionate permeability reduction mechanism on rupture of hydrogels performance,” *Colloids Surfaces A Physicochem. Eng. Asp.*, **560**(September 2018) 1–8 Elsevier (2019) doi:10.1016/j.colsurfa.2018.09.085
2) Y. Bai et al., “Experimental study of low molecular weight polymer/nanoparticle dispersed gel for water plugging in fractures,” *Colloids Surfaces A Physicochem. Eng. Asp.*, **551**(April) 95–107 Elsevier (2018) doi:10.1016/j.colsurfa.2018.04.067
3) B. R. Cancela et al., “Rheological study of polymeric fluids based on HPAM and fillers for application in EOR,” *Fuel*, **330**(May) 125647 Elsevier Ltd (2022) doi:10.1016/j.fuel.2022.125647
4) D. A. Z. Wever, F. Picchioni, and A. A. Broekhuis, “Polymers for enhanced oil recovery: A paradigm for structure-property relationship in aqueous solution,” *Prog. Polym. Sci.*, **36**(11) 1558–1628 Elsevier Ltd (2011) doi:10.1016/j.progpolymsci.2011.05.006
5) W. Pu et al., “A comprehensive review of polysaccharide biopolymers for enhanced oil recovery (EOR) from flask to field,” *J. Ind. Eng. Chem.*, **61** 1–11 The Korean Society of Industrial and Engineering Chemistry (2018) doi:10.1016/j.jiec.2017.12.034
6) Y. Fan, N. Boulif, and F. Picchioni, “Thermo-responsive starch-g-(PAM-co-PNIPAM): Controlled synthesis and effect of molecular components on solution rheology,” *Polymers (Basel).*, **10**(1) (2018) doi:10.3390/polym10010092
7) E. Czarnecka and J. Nowaczyk, “Semi-Natural superabsorbents based on Starch-g-poly(acrylic acid): Modification, synthesis and application,” *Polymers (Basel).*, **12**(8) (2020) doi:10.3390/polym12081794
8) J. Lee et al., “Preparation and characterization of superabsorbent polymers based on starch aldehydes and carboxymethyl cellulose,” *Polymers (Basel).*, **8**(6) 1–16 (2018) doi:10.3390/polym10060605
9) T. A. T. Mohd et al., “Properties of biodegradable polymer from terrestrial mushroom for potential enhanced oil recovery,” *Indones. J. Chem.*, **20**(6) 1382–1391 (2020) doi:10.22146/ijc.52254
10) K. Junlapong et al., “Effective adsorption of methylene blue by biodegradable superabsorbent cassava starch-based hydrogel,” *Int. J. Biol. Macromol.*, **158** 258–264 Elsevier B.V. (2020) doi:10.1016/j.ijbiomac.2020.04.247
11) S. Mishra et al., “Microwave assisted synthesis of polyacrylamide grafted starch (St-g-PAM) and its applicability as flocculant for water treatment,” *Int. J. Biol. Macromol.*, **48**(1) 106–111 Elsevier B.V. (2011) doi:10.1016/j.ijbiomac.2010.10.004
12) L. Li et al., “A novel treatment for amelioration of sludge dewaterability using green starch-grafted flocculant and realized mechanism,” *Sep. Purif. Technol.*, **301**(July) 122060 Elsevier B.V. (2022) doi:10.1016/j.seppur.2022.122060
13) J. Arayaphan et al., “Synthesis of photodegradable cassava starch-based double network hydrogel with high mechanical stability for effective removal of methylene blue,” *Int. J. Biol. Macromol.*, **168** 875–886 Elsevier B.V. (2021) doi:10.1016/j.ijbiomac.2020.11.166
14) K. C. Monyake and L. Alagha, “Enhanced separation of base metal sulfides in flotation systems using Chitosan-grafted-Polyacrylamides,” *Sep. Purif. Technol.*, **281**(June 2021) 119818 Elsevier B.V. (2022) doi:10.1016/j.seppur.2021.119818
15) P. Towongphaichayonte and R. Yoksan, “Water-

soluble poly(ethylene glycol) methyl ether-grafted chitosan/alginate polyelectrolyte complex hydrogels," *Int. J. Biol. Macromol.*, **179** 353–365 Elsevier B.V. (2021) doi:10.1016/j.ijbiomac.2021.03.026

16) K. Alharbi et al., "Controlled release of phosphorous fertilizer bound to carboxymethyl starch-g-polyacrylamide and maintaining a hydration level for the plant," *Int. J. Biol. Macromol.*, **116** 224–231 Elsevier B.V. (2018) doi:10.1016/j.ijbiomac.2018.04.182
17) T. Jiang et al., "Designing and application of reactive extrusion with twice initiations for graft copolymerization of acrylamide on starch," *Eur. Polym. J.*, **165**(January) 111008 Elsevier Ltd (2022) doi:10.1016/j.eurpolymj.2022.111008
18) S. Chami et al., "Polyacrylamide grafted xanthan: Microwave-assisted synthesis and rheological behavior for polymer flooding," *Polymers (Basel).*, **13**(9) 1–19 (2021) doi:10.3390/polym13091484
19) Q. Chen et al., "Synthesis and solution properties of a novel hyperbranched polymer based on chitosan for enhanced oil recovery," *Polymers (Basel).*, **12**(9) 1–24 (2020) doi:10.3390/POLYM12092130
20) S. Sinha, S. Mishra, and G. Sen, "Microwave initiated synthesis of polyacrylamide grafted Casein (CAS-g-PAM)-Its application as a flocculant," *Int. J. Biol. Macromol.*, **60** 141–147 Elsevier B.V. (2013) doi:10.1016/j.ijbiomac.2013.05.012
21) P. Wu et al., "Microwave assisted preparation and characterization of a chitosan based flocculant for the application and evaluation of sludge flocculation and dewatering," *Int. J. Biol. Macromol.*, **155** 708–720 Elsevier B.V. (2020) doi:10.1016/j.ijbiomac.2020.04.011
22) S. Mishra and K. Kundu, "Synthesis, characterization and applications of polyacrylamide grafted fenugreek gum (FG-g-PAM) as flocculant: Microwave vs thermal synthesis approach," *Int. J. Biol. Macromol.*, **141** 792–808 Elsevier LTD (2019) doi:10.1016/j.ijbiomac.2019.09.033
23) M. V. Nagarpita et al., "Synthesis and swelling characteristics of chitosan and CMC grafted sodium acrylate-co-acrylamide using modified nanoclay and examining its efficacy for removal of dyes," *Int. J. Biol. Macromol.*, **102** 1226–1240 Elsevier B.V. (2017) doi:10.1016/j.ijbiomac.2017.04.099
24) T. K. Giri, S. Pure, and D. K. Tripathi, "Synthesis of graft copolymers of acrylamide for locust bean gum using microwave energy: Swelling behavior, flocculation characteristics and acute toxicity study," *Polimeros*, **25**(2) 168–174 (2015) doi:10.1590/0104-1428.1717
25) M. Kaavessina, I. Fatimah, and S. Soraya, "Performance Test of Starch-g-Polyacrylamide Synthesized through Grafting as a Flocculant in Artificial Wastewater Treatment," *Equilib. J. Chem. Eng.*, **2**(1) 17 (2018) doi:10.20961/equilibrium.v2i1.40429
26) A. V. Singh, L. K. Nath, and M. Guha, "Microwave assisted synthesis and characterization of Phaseolus aconitifolius starch-g-acrylamide," *Carbohydr. Polym.*, **86**(2) 872–876 Elsevier Ltd. (2011) doi:10.1016/j.carbpol.2011.05.029
27) Y. You et al., "Synthesized cationic starch grafted tannin as a novel flocculant for efficient microalgae harvesting," *J. Clean. Prod.*, **344**(February) 131042 Elsevier Ltd (2022) doi:10.1016/j.jclepro.2022.131042
28) X. Chen et al., "Preparation of glycidyl methacrylate grafted starch adhesive to apply in high-performance and environment-friendly plywood," *Int. J. Biol. Macromol.*, **194**(September 2021) 954–961 Elsevier B.V. (2022) doi:10.1016/j.ijbiomac.2021.11.152
29) M. KT and S. P, "Characterization of Thermal and Physical properties of Biofield Treated Acrylamide and 2-Chloroacetamide," *Org. Chem. Curr. Res.*, **4**(3) 4–10 (2016) doi:10.4172/2161-0401.1000143
30) T. Lou et al., "Synthesis and flocculation performance of a chitosan-acrylamide-fulvic acid ternary copolymer," *Carbohydr. Polym.*, **170** 182–189 Elsevier Ltd. (2017) doi:10.1016/j.carbpol.2017.04.069
31) S. Distantina, F. Fadilah, and M. Kaavessina, "Swelling behaviour of kappa carrageenan hydrogel in neutral salt solution," *Int. J. Chem. Mol. Nucl. Mater. Metall. Eng.*, **10**(8) 917–920 (2016)
32) A. N. El-hoshoudy et al., "Experimental, modeling and simulation investigations of a novel surfmer-co-poly acrylates crosslinked hydrogels for water shut-off and improved oil recovery," *J. Mol. Liq.*, **277** 142–156 Elsevier B.V. (2019) doi:10.1016/j.molliq.2018.12.073
33) C. Durán-Valencia et al., "Development of enhanced nanocomposite preformed particle gels for conformance control in high-temperature and high-salinity oil reservoirs," *Polym. J.*, **46**(5) 277–284 (2014) doi:10.1038/pj.2013.99
34) A. Farasat et al., "Effects of reservoir temperature and water salinity on the swelling ratio performance of enhanced preformed particle gels," *Korean J. Chem. Eng.*, **34**(5) 1509–1516 (2017) doi:10.1007/s11814-017-0017-1
35) A. Z. Abidin, T. Puspasari, and H. P. R. Graha, "Utilization of cassava starch in copolymerisation of superabsorbent polymer composite (SAPC)," *J. Eng. Technol. Sci.*, **46**(3) 286–298 (2014) doi:10.5614/j.eng.technol.sci.2014.46.3.4
36) S. Li et al., "Enhancing oil recovery from high–temperature and high–salinity reservoirs with smart thermoviscosifying polymers: A laboratory study," *Fuel*, **288** (November 2020) 119777 Elsevier Ltd (2021) doi:10.1016/j.fuel.2020.119777
37) Y. Chen et al., "Insights into Enhanced Oil Recovery by Polymer-Viscosity Reducing Surfactant

Combination Flooding in Conventional Heavy Oil Reservoir," *Geofluids*, **2021** (2021) doi:10.1155/2021/7110414

38) A. Sabzian mellei et al., "Synergetic effects of PVP/HEC polymers on rheology and stability of polymeric solutions for enhanced oil recovery at harsh reservoirs," *J. Pet. Sci. Eng.*, **215**(PA) 110619 Elsevier B.V. (2022) doi:10.1016/j.petrol.2022.110619
39) S. M. Shehbaeverz and A. Bera, "Effects of nanoparticles, polymer and accelerator concentrations, and salinity on gelation behavior of polymer gel systems for water shut-off jobs in oil reservoirs," *Pet. Res.*,(xxxx) Chinese Petroleum Society (2022) doi:10.1016/j.ptlrs.2022.06.005